JOURNAL OF CATALYSIS 126, 219–227 (1990)

The Activity and Structure of Methanol Synthesis Catalysts Derived from Silver, Copper, and Cerium Alloys in Relation to Frost's Hypothesis

ELIZABETH A. SHAW, TREVOR RAYMENT, ANDREW P. WALKER, J. ROBERT JENNINGS,[1] AND RICHARD M. LAMBERT[2]

Department of Chemistry, University of Cambridge, Lensfield Road, Cambridge, England CB2 1EW

Received February 21, 1990; revised June 12, 1990

The structure and methanol synthesis activity of systems derived from binary cerium–silver and ternary cerium–silver–copper intermetallic precursors have been studied in the light of Frost's hypothesis according to which methanol synthesis occurs on a metal-promoted oxide phase. Results were obtained by *in situ* powder X-ray diffraction (XRD) with concurrent analysis of the exit gas stream by gas chromatography. To attain extensive metal/cerium oxide interaction, activation in N_2O and CO/H_2, with and without hydrogen pretreatment, was investigated; pressures up to 50 bar and temperatures up to 500°C were used. No methanol synthesis activity was observed from Ag/CeO_2 systems derived from binary cerium–silver alloys. Furthermore, the activity of the Cu/Ag catalyst derived from the ternary precursor was very significantly reduced relative to that expected by comparison with $CeCu_2$-derived catalysts on the basis of its copper content. Thus at least for methanol synthesis catalysts derived from these intermetallic precursors, the identity of the transition metal does indeed appear to be crucial.

INTRODUCTION

Methanol synthesis over $Cu/ZnO/Al_2O_3$ catalysts of the type used industrially has been much studied, and the reaction mechanism has been the subject of widespread debate. The fundamental questions at issue have included the nature of the active site and whether any particular synergy exists between the copper and the zinc oxide phases. The early work of Klier and coworkers suggested that the active site was composed of Cu(I) species dissolved in the zinc oxide matrix (*1–5*). This proposal however has been superceded, following work conducted by Chinchen *et al.* These workers demonstrated a linear relationship between methanol synthesis activity and total copper surface area for $Cu/ZnO/Al_2O_3$ catalysts (*6*). Furthermore, they found that copper supported on materials such as MgO and SiO_2 (*6*), and unsupported polycrystalline copper (*7*) had approximately the same turnover number as Cu/ZnO and $Cu/ZnO/Al_2O_3$ catalysts. These observations strongly suggest that the active centres are located exclusively on copper particles and that the oxide acts solely as a structural promoter. Yet the controversy has continued. Burch *et al.* examined Cu/ZnO, Cu/SiO_2, and Cu/ZrO_2 catalysts and demonstrated a clear support effect (*8, 9*), in agreement with the findings of Denise *et al.* (*10*). Burch also observed a synergic effect in physical mixtures of Cu/SiO_2 and ZnO/SiO_2 implying "synergy at a distance" (*9, 11*). Moreover, Frost has recently proposed a metal/oxide junction effect theory which could provide a unified view of all the different methanol synthesis catalysts (*12*). Within this theory, the chemistry occurs on the oxide phase. Frost indeed obtained active catalysts with thoria-supported Ag and Au—both metals

[1] I.C.I. plc, Chemicals & Polymers Group, Research Department, P.O. Box 90, Wilton, Middlesbrough, Cleveland TS6 8JE

[2] To whom correspondence should be addressed.

0021-9517/90 $3.00

normally regarded as inactive for methanol synthesis.

An alternative route to highly active methanol synthesis catalysts involves the use of lanthanide—copper intermetallic precursors (*13*), and a considerable amount of work has now been conducted on the structure and behavior of these materials (*14–17*). An *in situ* X-ray diffraction study with simultaneous measurement of catalyst activity by Nix *et al.* in this laboratory played an important part in this work (*15*). The phases identified in the active catalyst were metallic copper and rare earth oxide. This paper reports an extension in the use of this technique to an investigation of binary cerium–silver and ternary cerium–silver–copper precursors. A primary aim of the work was to obtain structure and activity data on Ag-containing materials, since such alloy-derived catalysts are known to generate extremely small metal particles which are in intimate contact with the support phase (*15, 18, 19*); the work was prompted by Frost's paper (*12*).

EXPERIMENTAL

The purpose-built sample cell used for *in situ* XRD/catalysis measurements has been used previously (*15, 18*) and was described in detail in the first publication. It has been used to pressures of 50 bar and temperatures of 500°C, and XRD data were collected using reflection geometry.

The intermetallic samples ($CeAg_2$, CeAg, CeM_2 [M = Cu : Ag, 2 : 1]) were prepared by electron beam fusion of the constituent metals under high vacuum as described earlier (*13*), with subsequent annealing at ~500°C for ~72 h. For each run, a catalyst charge of 0.05–0.20 g was crushed to a particle size of 50–250 μm and loaded into the reaction cell under an argon atmosphere. The cell was then sealed and transferred to the diffractometer. No bulk oxidation of the samples prior to activation was observed.

Gases were obtained from BOC Ltd. (Special Gases) and used without additional purification: hydrogen (CP grade, 99.999%), premixed $CO : H_2$ (33 : 67, impurities O_2 5 ppm, H_2O 2 ppm, and CO_2 20 ppm), nitrogen (CP grade, 99.999%), carbon monoxide (research grade, 99.95%), and premixed N_2O in He (2.6%, impurities O_2 6 ppm, CO_2 3 ppm, and H_2O 3 ppm). Flow rates of 10–20 standard cubic centimetres/min (sccm) were used. In most experiments the exit gas stream was sampled using on-line gas chromatography.

The XRD data were analysed by a variety of profile fitting techniques. For some of the systems investigated ($CeM_2/CO/H_2$ and $CeAg/N_2O$) only particle sizes based on the Scherrer equation using estimated FWHM values are reported; in these cases the low level of crystallinity resulted in data and subsequent fits which were not of sufficient quality for the application of more sophisticated methods of analysis for either ceria or transition metal particle sizes. In the case of $CeAg_2/CO/H_2$ and $CeAg/CO/H_2$, the counting statistics for CeO_2 were again poor and only particle sizes based on the Scherrer equation are given, but silver particle sizes deduced from the Scherrer equation using FWHM and integral breadths and from the Warren–Averbach method (applied to single lines) are listed (*20*). The standard used in the Warren–Averbach method of analysis was Ag powder (Johnson Matthey 120 mesh 99.9%) treated in H_2 at 200°C before use. Quantitative XRD analysis was performed by means of standard samples prepared as mechanical 1 : 1 and 1 : 2 molar mixtures of CeO_2 and Ag powders (CeO_2 Johnson Matthey 99.9%). Appropriate temperature and gas absorption corrections were made, giving an accuracy of better than 10% for the quantitative estimates.

RESULTS

$CeAg_2$ and CeAg Activation in CO/H_2 and H_2 + CO/H_2

The transformation of $CeAg_2$ in 50-bar CO/H_2 and the behavior of the transformed system at temperatures up to 500°C is illustrated by the sequence of diffraction patterns shown in Fig. 1. $CeAg_2$ exhibited much

lower reactivity to CO/H_2 than $CeCu_2$ (*15, 21*) despite adopting the same crystal structure (*22*). After prolonged exposure at 125°C diffraction peaks from the starting material still dominated the pattern. The transformation from the original alloy was completed at 150°C (the diffraction features of the starting material disappeared): cerium hydride and elemental silver were produced. Cerium hydride-to-oxide conversion occurred as the temperature was raised further and was complete by 250°C.

In Table 1 the average silver particle sizes deduced from the XRD data using various methods of particle size analysis as a function of temperature are given. At all temperatures, considerable discrepancies were observed between the results from the various methods. This is attributed to the presence of particles with a wide range of sizes, shown by the broad tails of the diffraction peaks. This implies that a profile analysis technique is needed to obtain a meaningful estimate of average particle size. The Warren–Averbach method applied to single lines is believed to give reliable estimates of average column lengths of these silver particles because size broadening effects greatly exceed any strain broadening effects in these systems. On the basis of FWHM values the average ceria particle size was ~65 Å. However, whereas silver peak intensities were of the same order as the integrated intensities obtained for the corresponding peaks in the diffraction pattern from a 1 : 2 mechanical mixture of CeO_2 and Ag powders, the ceria peak intensities were smaller by an order of magnitude.

TABLE 1

Silver Particle Sizes (in Angstroms)

T/°C	(111)			(200)			(220)		
	$D_{1/2}$	D_I	WA	$D_{1/2}$	D_I	WA	$D_{1/2}$	D_I	WA
				$CeAg_2 : CO/H_2$					
175	100	56	20				112	62	23
250	236	146	94	206	103	40	240	139	76
300	232	154	108	236	114	45	259	170	123
500	288	185	121	281	152	71	337	202	123
				CeAg : CO/H_2					
175	134	71	26				136	73	27
300	345	177	90	240	141	80	286	167	95

Note. Particle sizes deduced by ($D_{1/2}$) Debye–Scherrer equation using FWHM; (D_I) Debye–Scherrer equation using integral breadth; and (WA) Warren Averbach method.

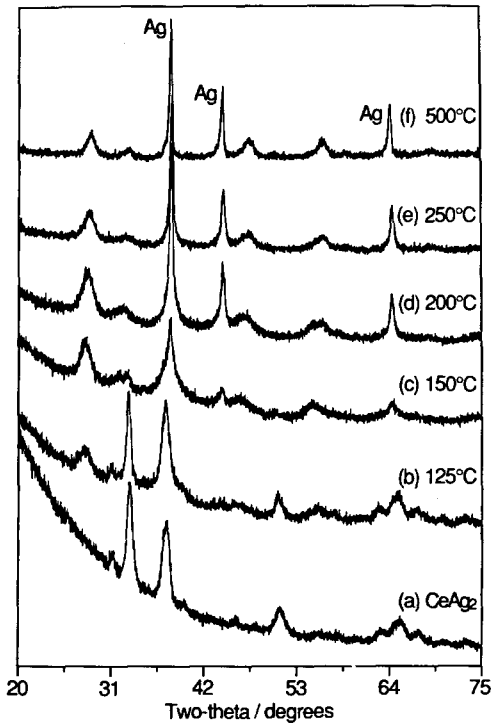

FIG. 1. Transformation of $CeAg_2$ in 50-bar CO/H_2 at increasing temperature. (a) $CeAg_2$, starting material; (b) 125°C; (c) 150°C; (d) 200°C; (e) 250°C; (f) 500°C.

No methanol production from CO/H_2 was detected below 300°C in this experiment, in marked contrast to the behaviour of $CeCu_2$ precursors (*15*) which yield highly active catalysts, *even under much milder conditions of activation* (15 bar, 100°C).

The behaviour of CeAg in 50-bar CO/H_2 was broadly similar to that of $CeAg_2$; after extensive treatment at 125°C, peaks from the starting material were still prominent in the diffraction pattern. Increasing the temperature directly to 250°C led to rapid conversion of the alloy producing elemental silver and cerium hydride. Cerium hydride-to-oxide conversion then ensued at this

temperature. When the temperature was stepped in 25°C increments from 125°C, conversion of the starting material was more gradual and a mixture of both cerium hydride and oxide together with elemental silver was produced. The cerium phase consisted mainly of oxide by 200°C but all traces of hydride were not lost until 300°C.

Data on silver particle sizes at temperatures of 175 and 300°C deduced from the latter experiment are included in Table 1. Broad particle size distributions are again noted. The Scherrer equation yielded a value of ~80 Å for the average particle size of ceria at 300°C. However, the intensity in the ceria reflections was only ~15% of that measured from the diffraction pattern obtained from a 1 : 1 mechanical mixture of CeO_2 and Ag powders. All the silver in the initial alloy was visible in the diffraction pattern. Again, no methanol production was detected at any stage during any of the experiments involving CeAg and CO/H_2 feed.

Nix *et al.* reported that prehydriding rare earth-Cu alloys in H_2 before switching to CO/H_2 could enhance the efficiency of catalyst activation (*15*). Consequently, further experiments were conducted with CeAg and $CeAg_2$ in which the starting alloys were treated with 50-bar pure H_2 before switching to the same pressure of CO/H_2. Both alloys were converted to cerium hydride and metallic silver; the transformation in H_2 was effected ~25°C lower than the temperature required for complete transformation of the alloy in the same pressure of CO/H_2. In CO/H_2 the main cerium hydride-to-oxide conversion proceeded at 200–300°C. The structures of the systems evolved were very similar to those produced by reaction in CO/H_2 alone. No methanol production from the CO/H_2 feed was observed.

CeAg Activation in N_2O

Silver of rather different structure was produced by oxidation of CeAg in N_2O. In Fig. 2 diffraction patterns obtained during and following the transformation of CeAg in 2.9-bar N_2O/He in an experiment in which

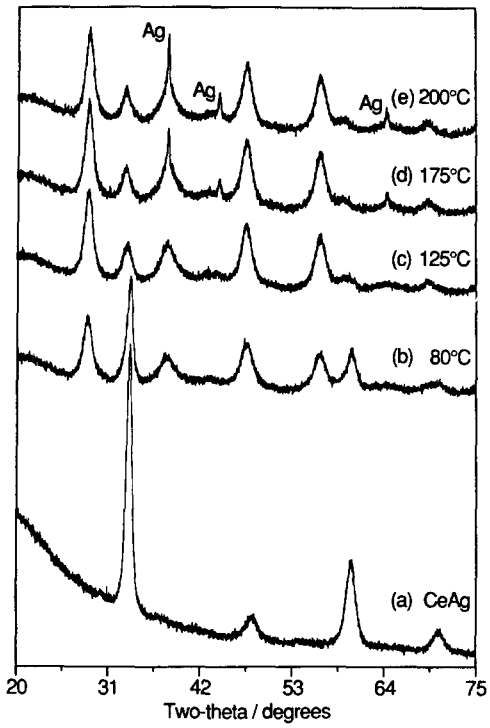

FIG. 2. Transformation of CeAg in 2.9-bar N_2O/He at increasing temperature. (a) CeAg, starting material; (b) 80°C; (c) 125°C; (d) 175°C; (e) 200°C.

the temperature was stepped gradually from room temperature to 200°C are shown. Conversion of the starting alloy to CeO_2 and Ag was completed at 125°C. Application of the Scherrer equation using the FWHM of the Ag(111) peak yielded an estimate of 40 Å for the average silver particle size. Approximately 30% of the silver was so highly dispersed that it was not seen in the diffraction patterns at all. The integrated intensities of the ceria reflections were only ~20% of those obtained for the corresponding peaks in the diffraction pattern obtained from the 1 : 1 mechanical mixture of CeO_2 and Ag powders, and the average particle size of the visible CeO_2 was estimated at ~65 Å. As the temperature was raised to 175–200°C sharp features emerged at the silver peak positions, essentially superimposed on the broad initial peaks. These sharp features correspond to the growth of some much big-

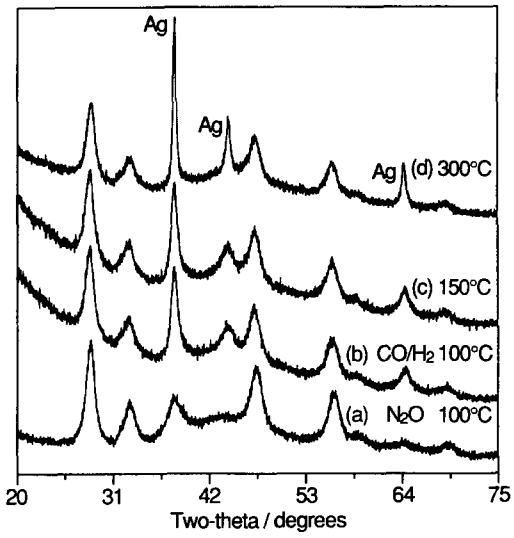

FIG. 3. Behavior of the Ag/CeO_2 system produced by reaction of CeAg in N_2O/He on raising the temperature in 50-bar CO/H_2. (a) N_2O, 100°C; (b) CO/H_2, 100°C; (c) 150°C; (d) 300°C.

ger silver particles; the line profiles indicate that a significant number of the very small silver particles produced initially were retained.

The effect of subsequent CO/H_2 treatment on the system produced by reaction of CeAg with N_2O is illustrated in Fig. 3. In this experiment transformation of the starting material in 2.9-bar N_2O/He was completed at 100°C, and the switch to 50-bar CO/H_2 was made at this same temperature. The diffraction pattern obtained in the hour immediately following the switch showed that CO/H_2 induced an immediate and pronounced sintering of the silver particles: the FWHM of the Ag(111) diffraction peak gave an estimated average silver particle size of 95 Å. All the silver in the initial alloy was visible in this diffraction pattern. Furthermore, compared to those observed following thermal sintering in N_2O, the line profiles of the "chemically sintered" material were more uniform. Additional growth of silver particles was observed upon raising the temperature and methanol synthesis activity was not observed at any temperature up to 300°C. Neither CO_2 nor H_2O evolution was detected following the switch to CO/H_2 feed. However, since gas chromatographic sampling occurred only every 40 min, transient production of CO_2 and/or H_2O could easily have been missed.

The observed sintering of the silver particles induced by the CO/H_2 gas mixture could not be prevented by performing the N_2O/He → CO/H_2 gas feed switch at room temperature, following conversion of the starting material in the N_2O/He mixture at 100°C. The onset of sintering was observed at temperatures between room temperature and 40°C. The effect was not noticeably pressure dependent: switching to 8-bar CO/H_2 had the same effect as switching to 50 bar of the mixture.

Experiments were also conducted in which, subsequent to oxidation of CeAg in N_2O, the temperature was lowered to room temperature and the gas feed then changed to 8 bar of pure H_2, pure CO, or pure N_2. In both reducing atmospheres the pattern of sintering observed in the mixed CO/H_2 feed was followed; in H_2 sintering was clearly observed even at room temperature, whereas the very small silver particles were stable to ~80°C in pure CO. In N_2 the onset of sintering was not observed until 175°C and in this case, the line profiles sharpened in the manner observed in the N_2O/He experiment.

CeM_2 Activation in CO/H_2 and H_2 + CO/H_2

In Fig. 4, diffraction patterns obtained during and following the transformation of CeM_2 in 50-bar CO/H_2 are shown. Transformation of the starting material occurred slowly at 150°C and was completed upon raising the temperature to 175°C. The crystallinity of the system produced by reaction of this alloy was extremely low; diffraction features were weak and broad but can be assigned to cerium hydride/oxide, silver, and copper phases. The cerium phase consisted mainly of hydride at 200°C, with conversion to oxide occurring on raising the

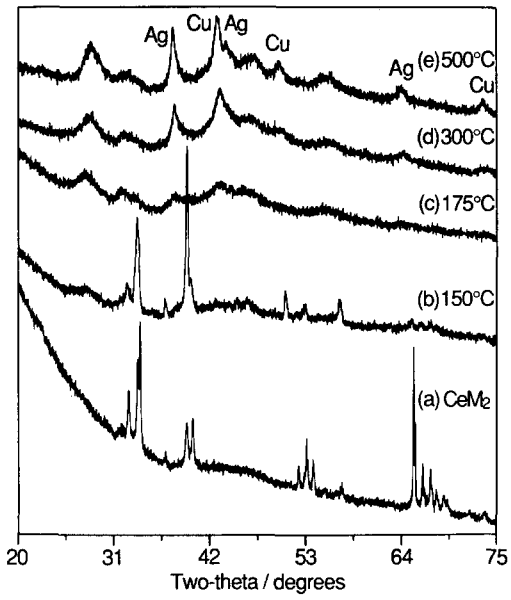

FIG. 4. Transformation of CeM_2 in 50 bar CO/H_2 at increasing temperature. (a) CeM_2, starting material; (b) 150°C; (c) 175°C; (d) 300°C; (e) 500°C.

temperature further. The low crystallinity of the system and the associated overlapping of diffraction peaks makes the extraction of any estimate of particle sizes particularly difficult here. Application of the Scherrer equation using FWHM gave an estimate of 40 Å for the average CeO_2 particle size, while an average silver particle size of ~80 Å at 250°C, increasing to 120 Å at 350°C was estimated from the Ag(111) peak.

In this case, some methanol synthesis activity was observed at temperatures of 225°C and above, falling away at 300°C. The level of methanol production was lower by at least a factor of 5 than that predicted on the basis of the copper content of the CeM_2 precursor by comparison with a catalyst derived from $CeCu_2$. Some methane formation was also detected at temperatures above 200°C.

In Fig. 5(I) further diffraction data for the temperature range 250–500°C are shown, following the transformation of CeM_2 in 50-bar CO/H_2 at lower temperatures. Figure 5(II) illustrates the changes in the integrated intensities of the silver and copper diffraction peaks between 250 and 450°C. In this experiment, a low level of methanol production was detected upon raising the temperature to 250°C. The level of methanol in the exit gas stream fell with time at this temperature but increased again upon raising the temperature to 300 and 350°C, though production fell rapidly to zero at this latter temperature. Thus, Fig. 5(II) implies that at least 20% of the metal was invisible to XRD at the temperatures at which methanol was produced. The changes in the diffraction pattern recorded at 500°C were due to the formation of some of the unidentified phase

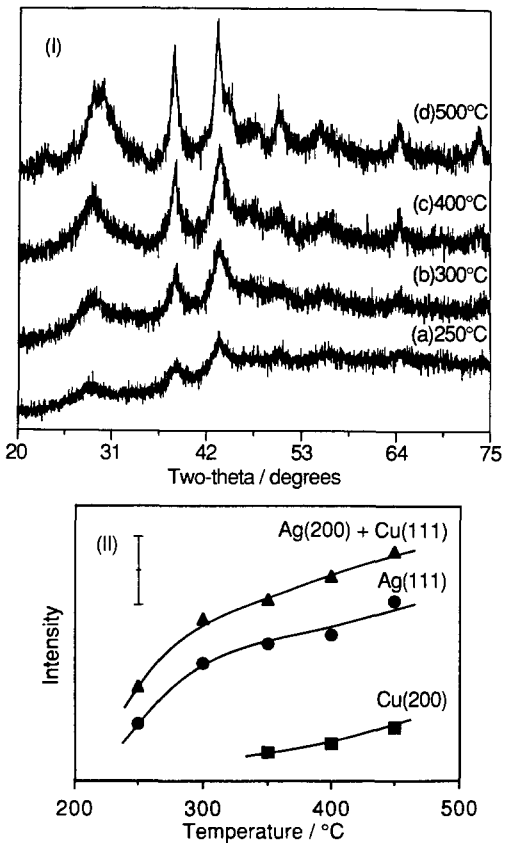

FIG. 5. (I) Behavior of the $Ag/Cu/CeO_2$ system produced by reaction of CeM_2 in 50 bar CO/H_2 on raising the temperature. (a) 250°C; (b) 300°C; (c) 400°C; (d) 500°C. (II) Increase in the integrated intensities of the silver and copper diffraction peaks between 250 and 450°C.

which was also produced at this temperature following activation of $CeCu_2$ at 50 bar (*21*).

The effect of hydrogen pretreatment at 50 bar on the activation of CeM_2 has also been investigated. The transformation of the starting alloy was not complete after prolonged treatment in H_2 at 125°C but conversion to a very poor crystalline mixture of cerium hydride and copper was completed upon raising the temperature in 50-bar CO/H_2. Cerium hydride-to-oxide conversion in this feed proceeded above 150°C, and the onset of a low level of methanol synthesis activity was detected at 200°C, i.e., 25°C lower than the temperature at which activity was observed without the hydrogen pretreatment.

DISCUSSION

Most discussions of the mechanism of methanol synthesis over Cu/oxide catalysts have taken the view that the Cu component plays an active role—in the metallic state, partially oxidised, or by incorporation into the host oxide lattice. A radically different hypothesis has been advanced by Frost (*12*) according to which all the chemistry occurs over the oxide phase, the function of the metal being to promote productivity of the oxide by enhancing the equilibrium concentration of ionised oxygen vacancies. It was proposed that this is achieved through the formation of Schottky junctions, so that any metal with a sufficiently large work function can therefore give rise to an active catalyst. The scheme also requires the metal/oxide contact area to be high.

Whether a Schottky junction is established at the metal/oxide interface depends on the disposition of the oxide conduction band edge relative to the metal Fermi level. A quantitative comparison of the Cu,Ag/ThO_2 (*12*) and Cu,Ag/CeO_2 systems would require an accurate knowledge of this property for the two types of system. This calls for accurate values of oxide workfunctions and band gaps. Unfortunately, for both ThO_2 and CeO_2, these quantities appear to be known either with considerable uncertainty or not at all, precluding such quantitative comparisons. (Indeed, Frost himself (*12*) carried out calculations for Cu/ZnO whereas his data refer to ThO_2-supported catalysts.)

Systems derived from activation of lanthanide–copper alloys are highly active for methanol synthesis from CO/H_2 (*13*). *In situ* XRD and microreactor studies (*15–17*) have led to the suggestion that the active site is associated with an intimate interaction between highly dispersed (XRD invisible) copper and the rare earth oxide phase. Quantitative XRD analysis of the catalyst derived from CO/H_2 activation of $CeCu_2$ indicated that ~60% of the copper present in the starting alloy was not seen in the diffraction pattern of the active catalyst and that about 80% of the cerium transformed to completely amorphous material (*21*). It is therefore conceivable that the mode of operation of these catalysts falls within the Frost mechanism. Indeed, some involvement of the oxide phase in the process of methanol synthesis was indicated by the observation that CO_2 poisoning was associated with conversion of the rare earth oxide surface into carbonate or bicarbonate (*16*).

In the present work no methanol synthesis activity was observed at temperatures up to 300°C from the CeO_2/Ag systems derived from activation of $CeAg_2$ and CeAg in CO/H_2 with or without H_2 pretreatment. It is noted that here, and indeed in all the systems reported in this paper, the observed ceria peaks corresponded to $\lesssim$20% of the cerium in the starting alloys; again most of the cerium existed in a completely amorphous phase. The structure of the metallic silver phase did differ from that of the copper in the systems evolved from $CeCu_2$. All the silver in the initial alloy was observed in XRD, and the particle sizes deduced from the Scherrer equation on the basis of the FWHM of the diffraction peaks were larger. Thus the extent of transition metal/oxide contact should be questioned. However, it remains true that the average metal particle size was still quite small. The Warren–Aver-

bach method estimated the average silver particle size at 250/300°C to be ≤100 Å. Since the particle size distributions were so wide, a considerable number of very small silver particles must have been present.

Use of an alternative activating atmosphere, N_2O in He, enabled CeAg to be transformed to CeO_2 and Ag at ≤100°C. Moreover, very highly dispersed silver was produced by this method with a significant portion even invisible to XRD. Despite the sintering observed on switching to a reducing gas environment and the accompanying increase in intensity of Ag diffraction peaks, these experiments generated small (~100 Å, Scherrer equation using FWHM) silver particles and an extremely poor crystalline cerium phase at temperatures where the systems derived from $CeCu_2$ are extremely catalytically active. There must have been substantial interaction between the silver and oxide phases, yet no methanol synthesis activity was observed. The pronounced structural changes accompanying the switch in feed gas to CO/H_2 could be associated with the removal of oxygen species (as CO_2, H_2O) from the surface or subsurface region of the silver particles (*23–25*); thus poisoning of the nascent catalyst by evolved CO_2 is a possibility (*13*).

The level of methanol synthesis activity observed from the ternary Cu–Ag–Ce alloy was significantly lower than that expected by comparison with the $CeCu_2$-derived catalyst on the basis of its copper content. Despite the silver being of extremely low crystallinity—some even invisible to XRD—it did not promote the activity of the system. On the contrary, an inhibiting role for silver must be postulated. Microreactor studies showed that the concentration of methanol in the exit gas stream following CO/H_2 activation of Ce : Cu : Ag 50 : 45 : 5 by weight at 200°C was 0.4% after 24 h (*26*); this may be compared with 3% after 200 h from Ce : Cu : Al 45 : 45 : 10 (*27*). Furthermore, the activity of a precipitated $Cu/ZnO/Al_2O_3$ catalyst in $CO/CO_2/H_2$ at 250°C *was reduced by 74% when 5% Ag was added* during catalyst preparation (*26*). A surface coating of copper particles with Ag provides a possible explanation of this effect since alloy formation between silver and copper is not known (*28*).

This work, therefore, provides no evidence to support Frost's theory. This is consistent with the earlier result that the activation energy for methanol synthesis over copper/rare earth oxide systems derived from a range of lanthanide–copper precursors was independent of the lanthanide component (*13*). It is important to remember, however, that the catalytic properties of these systems differ also from those of the industrial $Cu/ZnO/Al_2O_3$ catalysts. In particular, for the Cu/lanthanide oxide catalysts it was found that CO_2 acted as a poison rather than as a reactant (*13*) and that no correlation existed between catalyst activity and any estimate of copper surface area made from either XRD data (*15*) or from N_2O titration (*17*). Nevertheless, in both cases it appears that the identity of the metal is important in determining the catalytic properties; in neither case is the contribution and role of the support fully understood.

CONCLUSION

In the case of alloy-derived Ag/CeO_2 and $Ag,Cu/CeO_2$ methanol synthesis catalysts no evidence has been obtained in support of a hypothesis according to which the chemistry occurs solely on the oxide phase. This is despite generating systems characterized by intimate interactions between silver and oxide phases in which interface effects could be dominant. It seems that the chemical identity of the metal component in methanol synthesis catalysts is crucial, at least for catalysts produced from these intermetallic precursors.

ACKNOWLEDGMENTS

EAS and APW acknowledge the award of SERC Research Studentships. This work was supported by the provision of equipment under SERC Grant GR/D/25019. We are greatly indebted to Dr. G. Owen and Ms. D. Lloyd of ICI plc for preparation of the intermetallic samples, and to ICI plc for additional financial support. We thank Dr. W. Jones for loan of a gas chromatograph.

REFERENCES

1. Mehta, S., Simmons, G. W., Klier, K., and Herman, R. G., *J. Catal.* **57,** 339 (1979).
2. Himelfarb, P. B., Simmons, G. W., and Klier, K., *Amer. Chem. Soc. Div. Fuel Chem.* **29,** 233 (1984).
3. Dominguez, J. M., Simmons, G. W., and Klier, K., *J. Mol. Catal.* **20,** 369 (1983).
4. Herman, R. G., Klier, K., Simmons, G. W., Finn, B. P., Bulko, J. B., and Kobylinski, T. B., *J. Catal.* **56,** 407 (1979).
5. Parris, G. E., and Klier, K., *Amer. Chem. Soc. Div. Fuel Chem.* **29,** 218 (1984).
6. Chinchen, G. C., Waugh, K. C., and Whan, D. A., *Appl. Catal.* **25,** 101 (1986).
7. Chinchen, G. C., Spencer, M. S., Waugh, K. C., and Whan, D. A., *J. Chem. Soc. Faraday Trans. 1* **83,** 2193 (1987).
8. Bartley, G. J. J., and Burch, R., *Appl. Catal.* **43,** 141 (1988).
9. Burch, R., and Chappell, R. J., *Appl. Catal.* **45,** 131 (1988).
10. Denise, B., Sneedon, R. P. A., and Hamon, C., *J. Mol. Catal.* **17,** 359 (1982).
11. Burch, R., Chappell, R. J., and Golunski, S. E., *Catal. Lett.* **1,** 439 (1988).
12. Frost, J. C., *Nature (London)* **334,** 577 (1988).
13. Owen, G., Hawkes, C. M., Lloyd, D., Jennings, J. R., Lambert, R. M., and Nix, R. M., *Appl. Catal.* **33,** 405 (1987).
14. Hay, C. M., Jennings, J. R., Lambert, R. M., Nix, R. M., Owen, G., and Rayment, T., *Appl. Catal.* **37,** 291 (1988).
15. Nix, R. M., Rayment, T., Lambert, R. M., Jennings, J. R., and Owen, G., *J. Catal.* **106,** 216 (1987).
16. Jennings, J. R., Lambert, R. M., Nix, R. M., Owen, G., and Parker, D. G., *Appl. Catal.* **50,** 157 (1989).
17. Nix, R. M., Judd, R. W., Lambert, R. M., Jennings, J. R., and Owen, G., *J. Catal.* **118,** 175 (1989).
18. Walker, A. P., Rayment, T., and Lambert, R. M., *J. Catal.* **117,** 102 (1989).
19. Walker, A. P., Rayment, T., Lambert, R. M., and Oldman, R. J., *J. Catal.* **125,** 67 (1990).
20. Delhez, R., de Keijses, Th. H., and Mittemeijer, E. J., *Fresenius Z. Anal. Chem.* **312,** 1 (1982).
21. Shaw, E. A., Rayment, T., Walker, A. P., and Lambert, R. M., submitted for publication.
22. Iandelli, A., and Palenzona, A., *in* "Handbook of the Physics and Chemistry of Rare Earths" (K. A. Gschneidner, Jr., and L. Eyring, Eds.), Vol. 2. North-Holland, Amsterdam, 1979.
23. Scholten, J. J. F., Konvalinka, J. A., and Beekman, J. W., *J. Catal.* **28,** 209 (1973).
24. Seyedmonir, S. R., Strohmayer, D. E., Geoffroy, G. L., Vannice, M. A., Young, H. W., and Linowski, J. W., *J. Catal.* **87,** 424 (1984).
25. Lefferts, L., Van Ommen, J. G., and Ross, J. R. H., *J. Catal.* **114,** 303 (1988).
26. Jennings, J. R., unpublished data.
27. Owen, G., Hawkes, C. M., Lloyd, D., Jennings, J. R., Lambert, R. M., and Nix, R. M., *Appl. Catal.*, **58,** 69 (1990).
28. "Constitution of Binary Alloys" (M. Hansen, Ed.). McGraw-Hill, New York, 1958.